Large Step Shear Strain Experiments with Parallel-Disk Rotational Rheometers*

PAUL R. SOSKEY,† *Department of Polymer Science and Engineering, University of Massachusetts, Amherst, Massachusetts 01003* and H. HENNING WINTER, *Department of Chemical Engineering and Department of Polymer Science and Engineering, University of Massachusetts, Amherst, Massachusetts 01003*

Synopsis

A new method is proposed and tested for step shear strain experiments with parallel-disk rotational rheometers. The method is applicable to large strains, i.e., outside the linear viscoelastic region. The nonhomogeneity of the strain in the parallel-disk rheometer is accounted for by a correction term which is similar to the well-known Rabinowitsch correction in capillary rheometry. The transient shear relaxation moduli of a low-density polyethylene (150°C) and of a polystyrene (180°C) from this method agree very well with equivalent data fron a cone-and-plate rheometer. The two different geometries give an overlapping set of data; small-strain data ($\gamma = 0.1-5$) from cone-and-plate and large-strain data ($\gamma = 0.4-25$) from parallel disk. The step strain data support the separability of the relaxation modulus into time- and strain-dependent functions. The strain dependence is well approximated by a sigmoidal function. The data were obtained with a Rheometrics dynamic spectrometer having a maximum angular displacement of 0.5 rad.

INTRODUCTION

The step shear strain experiment is a direct means of measuring the strain-dependent rheology of polymeric liquids.[1,2] In the experiment, a sample of the polymeric liquid is placed into a shear rheometer and the system is kept at rest until the sample is completely relaxed to the stress-free state. At time $t = 0$, a finite shear strain of magnitude γ_{21} is "instantaneously" applied which results in a stress in the sample. The stress is measured as it relaxes with time while the strain of the sample is held constant

*Dedicated to Prof. H. Janeschitz-Kriegl on his 60th birthday.

†Current address: Union Carbide, Polyolefin Division, Bound Brook, NJ.

 Published by John Wiley & Sons, Inc.
Journal of Rheology, 28(5), 625–645(1984) CCC 0148-6055/84/050625-23$04.00

at all times $t > 0$. The result of the measurement is a time- and strain-dependent shear relaxation modulus

$$G(t,\gamma) = \tau_{21}(t,\gamma)/\gamma_{21}, \tag{1}$$

where τ_{21} is the shear stress.

The corresponding transient first normal stress difference has been discussed by Lodge and Meissner[3] who predict that the ratio of the transient first normal stress difference to the transient shear stress equals the shear strain and is independent of time. This relationship has been verified experimentally for several polymeric liquids.[4-7] In this study, we have limited our discussion to the relaxation of the shear stress. Our approach can also be applied to the derivation of a correction method for the first normal stress difference.

The step strain experiment is also a direct method of measuring the linear viscoelastic relaxation modulus of polymeric liquids. In the limit of small strain, the shear stress is described by a linear viscoelastic model[8]

$$\tau_{21}(t) = \int_{-\infty}^{t} \sum_{i=1}^{N} \frac{g_i}{\lambda_i} e^{(t-t')/\lambda_i} \gamma_{21}(t',t)\, dt'. \tag{2}$$

This model predicts that the relaxation modulus, Eq. (1), is independent of the shear strain $\gamma_{21}(t',t)$:

$$\overset{\circ}{G}(t) = \sum_{i=1}^{N} g_i e^{-t/\lambda_i}. \tag{3}$$

The choice of a discrete relaxation spectrum, g_i and λ_i, is made here for simplification; it will not affect the arguments below. In the following we will call a step strain "large" if the corresponding relaxation modulus is a function of time *and* strain.

Previously, the large step strain test has been performed in rheometers in which the test sample is subjected to a *homogeneous* strain. Such rheometers are the cone-and-plate rotational rheometer,[1,2,4,9-11] the sandwich device,[6,7] and, to a good approximation, the Couette system.[5,12] An alternative method is proposed here for rotational rheometers which are limited in their angular displacement. The main reason for developing this new method is the need for a large strain.

The rotational rheometer in our laboratory has a drive system with a maximum angular displacement $\theta_{max} = 0.5$ rad. For the

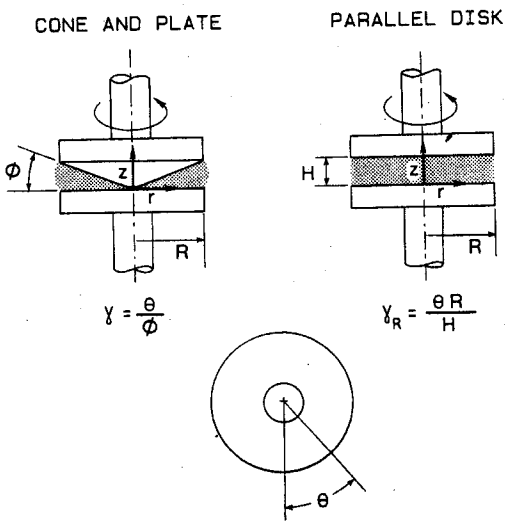

Fig. 1. Sketch of cone-and-plate and parallel-disk geometries.

cone-and-plate geometry (Fig. 1), with a cone angle $\phi = 0.1$ rad, the maximum strain obtainable is

$$\gamma_{max} = \theta_{max}/\phi = 5. \tag{4}$$

This strain, although outside the linear viscoelastic region, is relatively small. It can be increased by choosing smaller cone angles. Lin[11] obtained large step strain data with a cone angle $\phi = 0.018$ rad. However, small cone angles (below 0.1 rad for a modified Weissenberg rheometer) were found to cause errors in transient stress measurements.[13] The errors were attributed to the lack of stiffness of the rheometer against axial forces which originate from the normal stress in the sheared liquid. These errors were severe for the normal stress measurement, but they seem to be tolerable for the shear stress.

Another way to increase the magnitude of the strain for an instrument with limited angular displacement is to use the parallel-disk geometry, as shown in Figure 1, and to decrease the gap thickness. We prefer this second method, since (1) it does not require many cones having different angles, (2) the sample preparation is simpler for the parallel-disk system, (3) the rise time in step strain can be made uniform for all strains, and (4) the sen-

sitivity to errors in gap setting is reduced. The problem of the parallel-disk experiment is the nonhomogeneous strain of the sample.

CORRECTION FOR NONHOMOGENEOUS STRAIN

The transient torque response has to be corrected for the nonhomogeneous strain. The correction method is similar to the one of Rabinowitsch[14] for evaluating steady shear flow in capillary rheometers. It also applies to steady shear flow in a parallel-disk rheometer.[15] These corrections apply to *steady-state* shear flow; whereas the correction discussed here has to accommodate the *transient* response of the step strain.

The analysis is based on the assumptions that inertial effects and viscous heating in the sample are negligible and also, more importantly, that for the parallel-disk geometry (Fig. 1) the planes in the z direction are shear planes (i.e., the material planes parallel to the boundary disks move rigidly). Thus, the shear strain increases linearly in the radial direction:

$$\gamma_{z\theta}(r,t) = \theta(t)r/H, \qquad 0 < r < R, \tag{5}$$

and is the same in each of the shear planes ($\gamma_{z\theta}$ independent of z). Edge effects at $r = R$ are also neglected. H is the gap (and sample) thickness and $\theta(t)$ is the relative angular displacement of the disks. In the step strain experiment, the angular displacement is a constant, θ_0, at $t > 0$. The finite rise time of the strain is assumed to be negligibly short. The shear strain is independent of time during the stress relaxation:

$$\gamma_{z\theta}(r) = r\theta_0/H = \gamma_R r/R, \qquad 0 < t, \tag{6}$$

where γ_R is the strain at the outer edge of the disks. The total transient torque is

$$\mathcal{T}(t,\gamma_R) = 2\pi \int_0^R \tau_{z\theta}(r,t)r^2\, dr, \quad 0 < t. \tag{7}$$

By substitution of the shear stress with the shear relaxation modulus [Eq. (1)] and a change of variables according to Eq. (6), the following relation is obtained:

$$\mathcal{T}(t,\gamma_R) = \frac{2\pi R^3}{\gamma_R^3} \int_0^{\gamma_R} G(t,\gamma)\gamma^3\, d\gamma. \tag{8}$$

After differentiation with respect to γ_R, Eq. (8) becomes

$$G(t,\gamma_R) = \frac{2\mathcal{T}(t,\gamma_R)}{\pi R^3 \gamma_R}\left(\frac{3}{4} + \frac{1}{4}\frac{\partial \ln[2\mathcal{T}(t,\gamma_R)/\pi R^3]}{\partial \ln \gamma_R}\right). \quad (9)$$

In the linear viscoelastic limit, the torque is proportional to the strain γ_R and the magnitude of the term in brackets reduces to unity. In the limit of small strain, the linear viscoelastic modulus measured by parallel disks is

$$\mathring{G}(t) = \lim_{\gamma_R \to 0} G(t,\gamma_R) = \frac{2\mathcal{T}(t,\gamma_R)}{\pi R^3 \gamma_R}. \quad (10)$$

Therefore, we define an apparent relaxation modulus for step strain in the parallel-disk geometry:

$$G_a(t,\gamma_R) \equiv 2\mathcal{T}(t,\gamma_R)/\pi R^3 \gamma_R \quad (11)$$

which is *obtained directly from each relaxation experiment.* The term in large parentheses in Eq. (9) becomes, after substitution with the apparent relaxation modulus,

$$\chi(t,\gamma_R) = 1 + \frac{1}{4}\frac{\partial \ln G_a(t,\gamma_R)}{\partial \ln \gamma_R}. \quad (12)$$

This correction term is determined from a set of relaxation experiments at different magnitudes of γ_R. The resulting equation for the correction due to nonhomogeneous strain is

$$G(t,\gamma_R) = G_a(t,\gamma_R)\left(1 + \frac{1}{4}\frac{\partial \ln G_a(t,\gamma_R)}{\partial \ln \gamma_R}\right). \quad (13)$$

It should be noted that the derivation of Eq. (13) follows directly from a balance of forces. No specific type of constitutive equation is assumed.

EXPERIMENTAL

Two polymer melts were investigated: a low-density (high-pressure) polyethylene (LDPE) (duPont Alathon 20, M_n = 25,000, M_w = 200,000) and a polystyrene (PS) (Dow Styron 666, M_n = 90,000, M_w = 220,000). These two samples were chosen to test our method on a polymer having long-chain branched molecules and one with linear molecules.

A rotational rheometer (Rheometrics dynamic spectrometer, RDS) was used for both the oscillatory shear and step shear strain experiments. The geometries of the test fixtures were cone and plate (D = 25 mm, ϕ = 0.1 rad) and parallel disks (D = 25 mm). Having been designed primarily for oscillatory experiments requiring small strains ($\gamma < 0.5$), the rheometer produces a maximum angular displacement of only 0.5 rad. The transducer measures a maximum torque of 0.2 N m.

LINEAR VISCOELASTIC CHARACTERIZATION

Oscillatory shear experiments at small strain were performed to determine the storage modulus $G'(\omega)$ and the loss modulus $G''(\omega)$ as a function of angular frequency in the range $0.1 < \omega < 100$ rad/s. The experiments were performed at several temperatures and the resulting curves were shifted to a reference temperature (150°C for LDPE and 180°C for PS), using the principle of time/temperature superposition.[8] The shifted data are given in Figure 2.

The parameters of a discrete relaxation time spectrum were obtained by fitting both the storage and the loss moduli,[4]

$$G'(\omega) = \sum_{i=1}^{N} g_i \frac{\lambda_i^2\omega^2}{1 + \lambda_i^2\omega^2}, \qquad G''(\omega) = \sum_{i=1}^{N} g_i \frac{\lambda_i\omega}{1 + \lambda_i^2\omega^2} \quad (14)$$

Discrete values of λ_i and g_i were determined with a finite difference Levenberg–Marquardt routine[16] and are listed in Table I. The full lines in Figure 2 were calculated according to Eq. (14), using the values in Table I.

Large-Strain Experiments

Large step shear strain experiments were performed at varying finite strains. The strains obtained for the various geometries appear in Table II. Values of γ_R with the parallel-disk geometry were chosen to overlap the range of strain obtained with the cone-and-plate geometry.

A finite rise time Δt is required for the motor to rotate the upper disk to the prescribed angle θ_0. Figure 3 shows the transient angular displacement. The rise time should be as small as

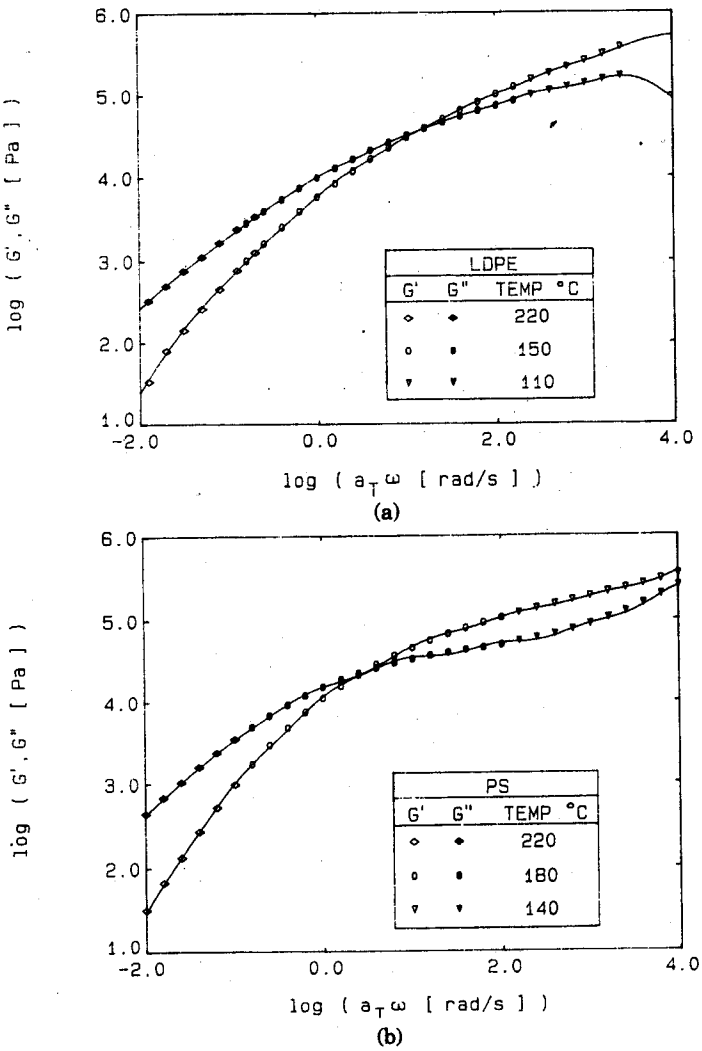

Fig. 2. Storage and loss moduli as functions of reduced angular frequency. The solid lines were calculated from Eq. (14) using the constants of Table I. (a) LDPE, reference temperature T_0 = 150°C, (b) PS, reference temperature T_0 = 180°C.

TABLE I
Discrete Relaxation Time Spectra of LDPE and PS Samples

LDPE (T_0 = 150°C)		PS (T_0 = 180°C)	
λ_i [s]	g_i [Pa]	λ_i [s]	g_i [Pa]
5.913×10^{1}	3.776×10^{1}	5.152×10^{1}	7.763×10^{1}
1.817×10^{1}	3.710×10^{2}	8.669×10^{0}	1.338×10^{3}
3.680×10^{0}	1.952×10^{3}	5.135×10^{0}	9.275×10^{2}
6.606×10^{-1}	1.085×10^{4}	1.018×10^{0}	1.762×10^{4}
1.073×10^{-1}	2.806×10^{4}	1.107×10^{-1}	5.004×10^{4}
2.060×10^{-2}	6.040×10^{4}	1.065×10^{-2}	6.978×10^{4}
3.026×10^{-3}	1.371×10^{5}	9.927×10^{-4}	1.009×10^{5}
3.381×10^{-4}	3.027×10^{5}	5.821×10^{-5}	5.558×10^{5}

possible in order to avoid corrections to the relaxation modulus at intermediate times.[4] An important observation is that the rise time was proportional to the angular displacement and independent of the torque which changed with gap setting and sample. The rise time never exceeded 55 ms, even at the largest strain, $\gamma = 25$.

The stress response to the step strain is shown in Figure 4 in the form of transient moduli. For the cone-and-plate geometry, the true relaxation modulus is plotted, while for the parallel-disk geometry the apparent relaxation modulus, Eq. (11), is plotted. The flat regions at short times occur because the transducer was overloaded at the beginning of the experiment. This overload also resulted in an offset at long times (about 0.5% of the transducer range) which is evident in the gradual leveling off of the relaxation modulus. Even though the data were corrected for this offset, results beyond 10 s have substantial scatter due to the inac-

TABLE II
Range of Strains Experimentally Obtained in RDS

Geometry	Gap (mm)	Strain
Cone and plate	—	$0.1 < \gamma < 5$
Parallel disk	1.00	$0.4 < \gamma_R < 4.5$
	0.50	$1 < \gamma_R < 12$
	0.25	$5 < \gamma_R < 25$

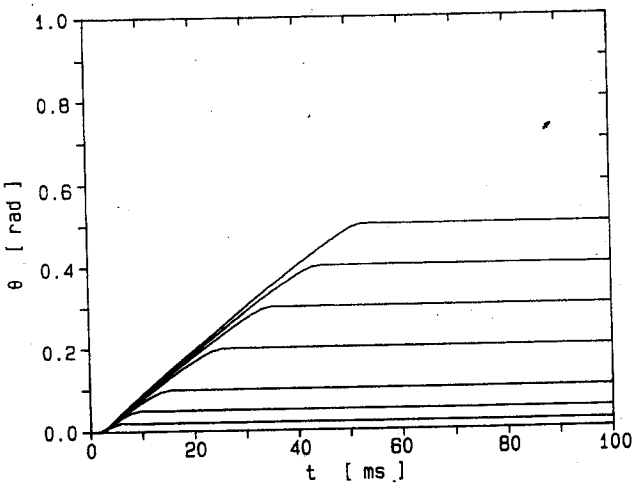

Fig. 3. Measured angular displacement as a function of time for step strain experiment on RDS.

curacy of the transducer at torque levels less than 5×10^{-4} N m. Therefore, reliable data were obtained over two time decades, $0.1 < t < 10$ s. The correction of the parallel-disk data for the nonhomogeneous strain is discussed in the next section.

RESULTS AND DISCUSSION

To obtain the true transient shear relaxation modulus at large strains, the apparent modulus has been corrected according to Eq. (13). First, the apparent modulus was plotted against the shear strain γ_R with time as a parameter (see Fig. 5). The solid curves were determined by fitting the experimental points to a third-order polynomial.[17] The slope of these curves was used in Eq. (12) to determine the correction factor $\chi(t,\gamma_R)$. At small strains, the slope of the curves is zero and the correction factor approaches unity, $\chi = 1$. At larger strains, the slope becomes increasingly negative. No limiting slope was observed for the range of the shear strains studied. The corrected relaxation moduli and the apparent moduli are compared in Figure 6. At large strains, the corrected moduli are significantly lower than the apparent moduli.

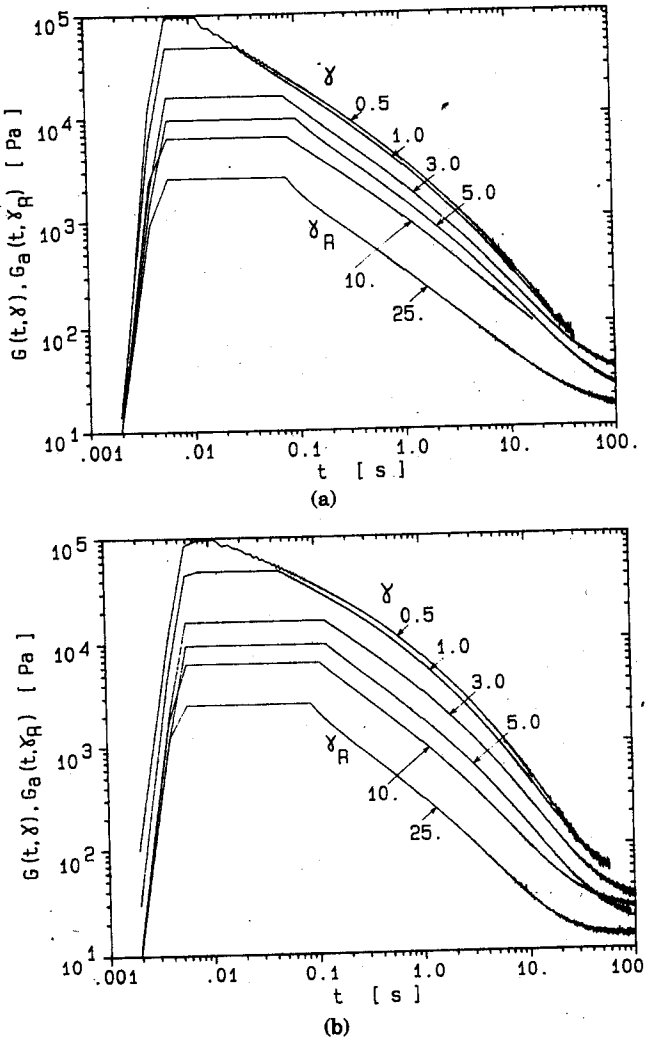

Fig. 4. Transient shear relaxation modulus plotted directly by rheometer. $G(t,\gamma)$ is plotted for cone-and-plate geometry ($0.5 \leq \gamma \leq 5.0$). $G_a(t,\gamma_R)$ is plotted for parallel disk (γ_R = 10 and 25). (a) LDPE, T = 150°C, (b) PS, T = 180°C.

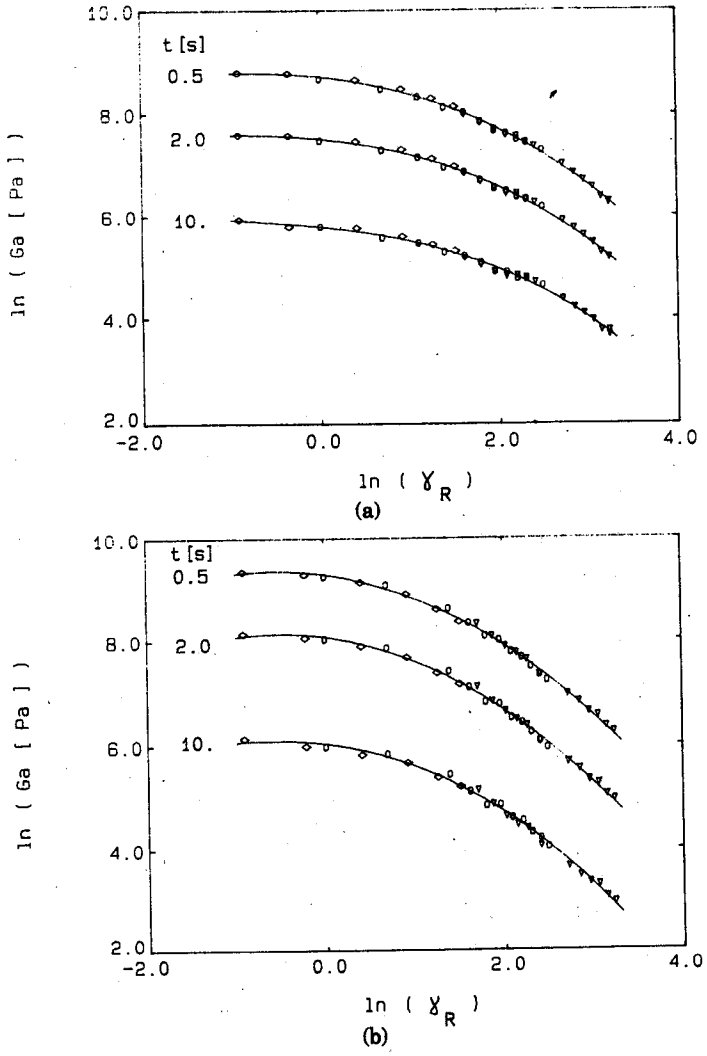

Fig. 5. Apparent modulus as a function of strain from parallel-disk experiments. (▽) 0.25-mm, (○) 0.50-mm, (◇) 1.00-mm gap. The solid lines were fit by a third-order polynomial. (a) LDPE, T = 150°C, (b) PS, T = 180°C.

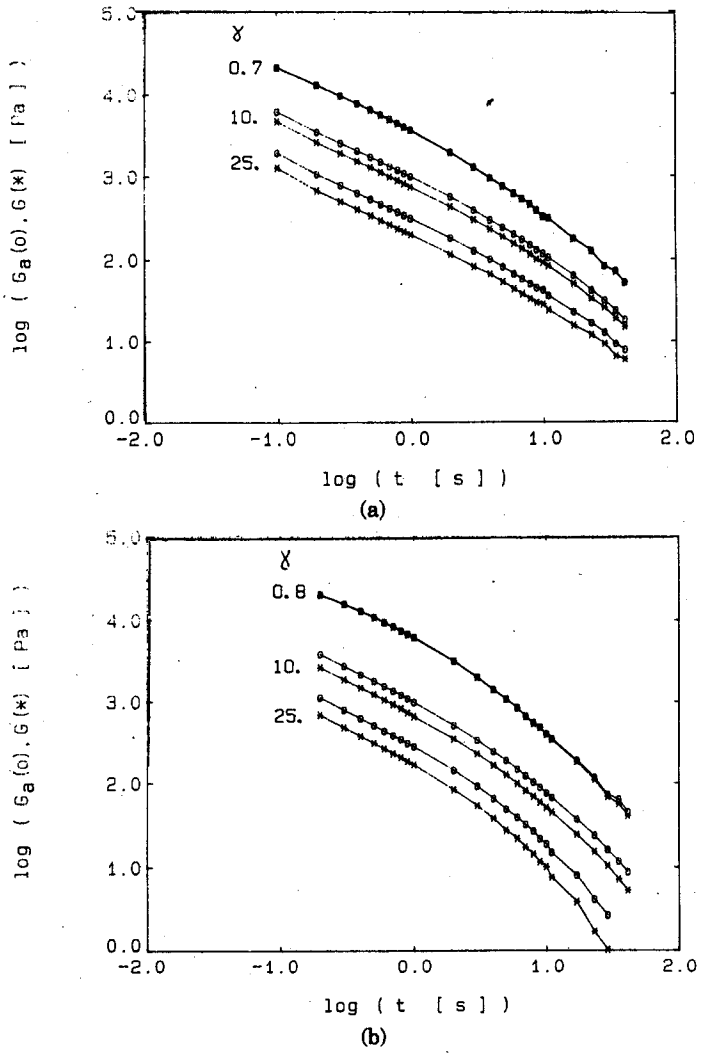

Fig. 6. Correction of transient apparent shear relaxation modulus for non-homogeneous strains. (-O-) $G_a(t,\gamma_R)$, (-*-) $G(t,\gamma)$, solid lines just connect individual data points. (a) LDPE, T = 150°C, (b) PS, T = 180°C.

The relaxation moduli determined from the nonhomogeneous strain in the parallel disk agree well with the relaxation moduli which were obtained from the cone-and-plate geometry. Figure 7 shows a superposition of the two sets of experimental data.

Several of the measured relaxation moduli, from both geometries, are shown in Figure 8. The solid line is the relaxation modulus of linear viscoelasticity as calculated from Eq. (3) and the relaxation spectrum of Table I. The oscillations in the calculated curve are due to the choice of a discrete spectrum. The data at the lowest strain, $\gamma = 0.2$, is described well by the linear viscoelastic model.

Nonlinear viscoelastic theory of polymeric liquids,[18] as applied to step shear,[7,11] suggests that the shear relaxation modulus can be factorized into a time-dependent function, the linear viscoelastic modulus $\mathring{G}(t)$, and a strain function $h(\gamma)$:

$$G(t,\gamma) = \mathring{G}(t)\, h(\gamma). \tag{15}$$

The strain function approaches unity at small strains and decreases monotonically as the strain increases.

The strain function of the two polymers has been determined by shifting the curves of Figure 8 vertically upward until they coincide with the linear viscoelastic curve. The magnitude of the shift, $h(\gamma)$, is plotted in Figure 9. The parallel-disk data agree well with the cone-and-plane data at lower strains and continue in a smooth fashion to the large-strain region. The PS exhibits much stronger strain dependence than the LDPE.

Several forms of equations have been proposed for fitting the strain function data. Wagner[19] proposed a single exponential, while Osaki[20] and Laun[4] used a sum of two exponential functions of the form

$$h(\gamma) = f \exp(-n_1\gamma) + (1 - f) \exp(-n_2\gamma). \tag{16}$$

The single exponential form does not describe the large-strain region as it underpredicts the data. The double exponential form gives a good fit at the larger strains but underpredicts at the small-strain region where the data approach unity in a sigmoidal fashion. A sigmoidal form has been proposed by Papanastasiou et al.[21]

$$h(\gamma) = 1/(1 + a\gamma^2). \tag{17}$$

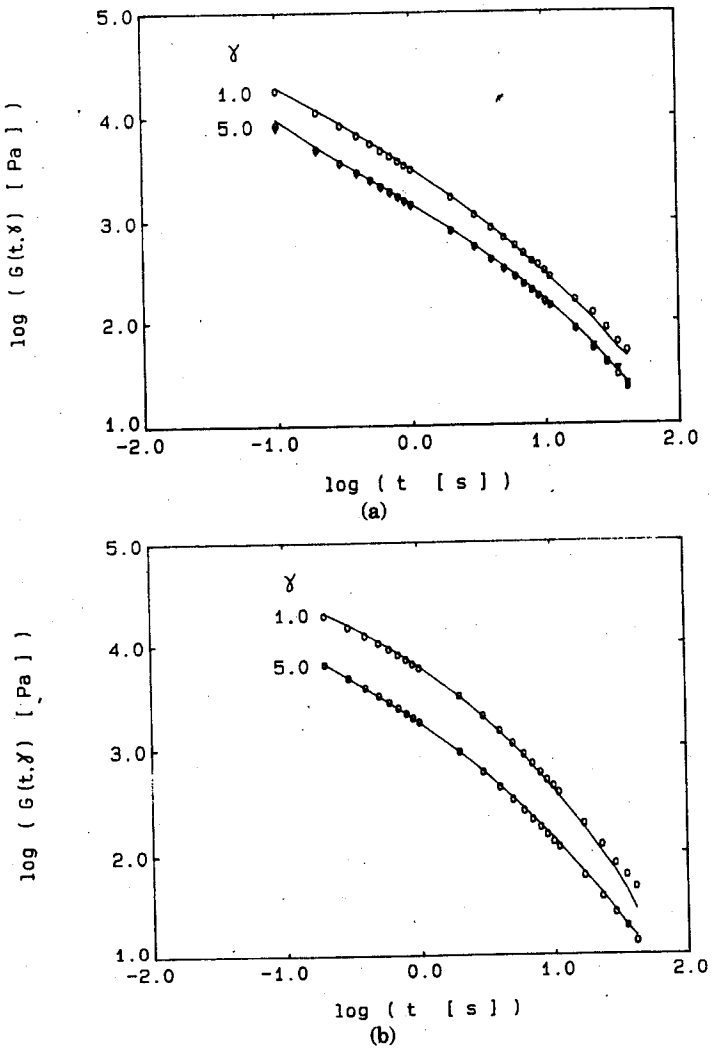

Fig. 7. Comparison between shear relaxation modulus measured with parallel disks, (▽) 0.25-mm and (○) 0.50-mm gap, and measured with cone and plate (—). (a) LDPE, T = 150°C, (b) PS, T = 180°C.

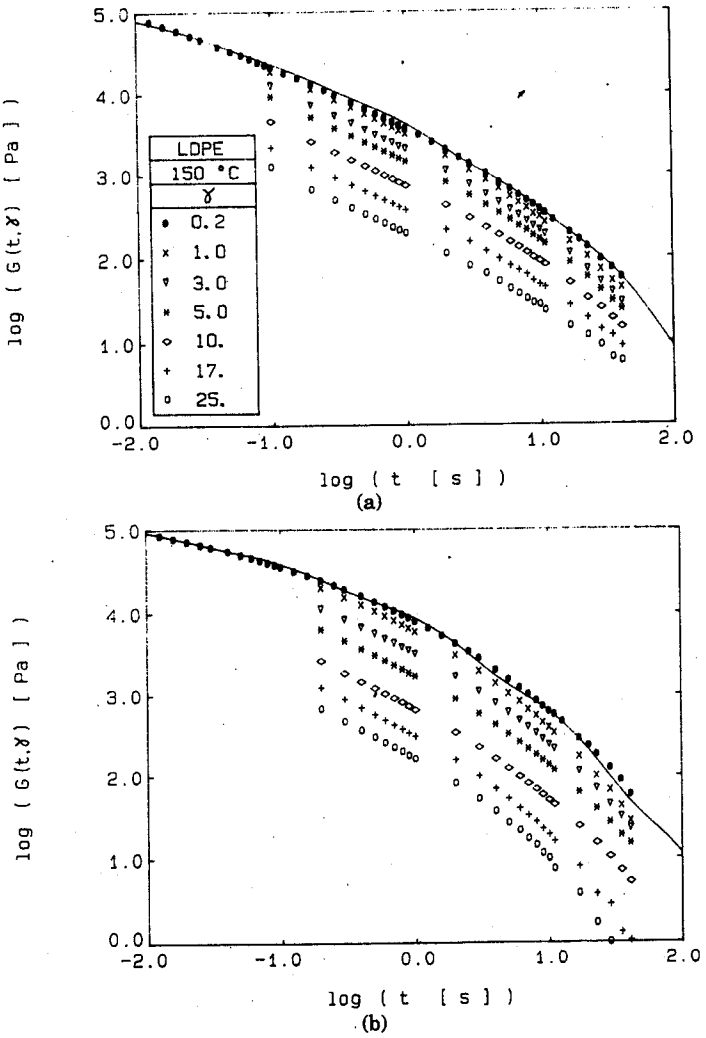

Fig. 8. Transient shear relaxation modulus at different shear strains. The solid line is the transient shear relaxation modulus of linear viscoelasticity calculated from Eq. (3) using the constants of Table II. (a) LDPE, T = 150°C, (b) PS, T = 180°C. γ = (●) 0.2, (×) 1.0, (▽) 3.0, (*) 5.0, (◇) 10., (+) 17., (○) 25.

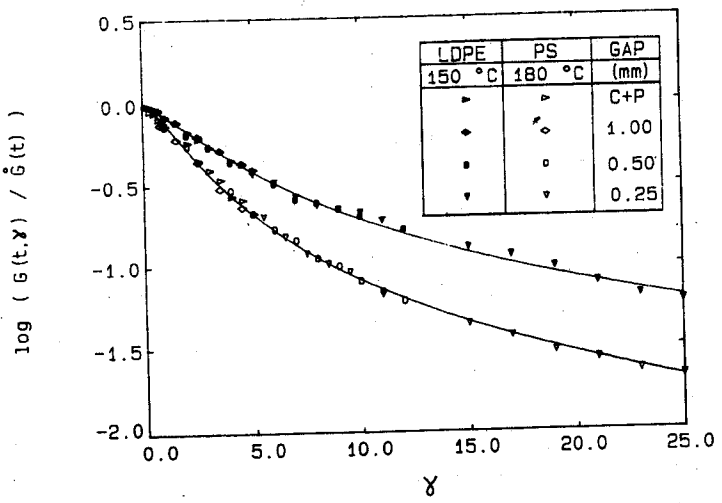

Fig. 9. Strain function $h(\gamma) = G(t,\gamma)/\hat{G}(t)$ for LDPE, $T = 150°C$ (filled symbols) and PS, $T = 180°C$ (open symbols). The solid lines were calculated from Eq. (18) using the parameters in Table III.

This function has a sigmoidal shape but, due to the choice of γ^2 in the denominator, the experimental data are overpredicted at low strains and underpredicted at high strains. For a better fit of the data, we propose a function where the exponent of the shear strain (or a significant strain tensor invariant[21]) is a material parameter:

$$h(\gamma) = 1/(1 + a\gamma^b). \tag{18}$$

This form still contains the sigmoidal nature of Eq. (17) yet fits the data much better over the entire strain region. The parameter values of the different approximations appear in Table III. The fit according to Eq. (18) is shown in Figure 9. For clarity, the comparison between the different forms of strain function approximations is shown in a separate figure, Figure 10. The sum of two exponential functions and the sigmoidal function is found to describe the shear data equally well.

TABLE III
Parameters for Approximation of Measured Strain Function

Approximation function	Parameters	LDPE (150°C)	PS (180°C)
$h(\gamma) = f\exp(-n_1\gamma) + (1-f)\exp(-n_2\gamma)$ (ref. 20)	f	0.67	0.88
	n_1	0.304	0.377
	n_2	0.070	0.073
$h(\gamma) = 1/(1+a\gamma^2)$ (ref. 21)	a	0.043	0.124
$h(\gamma) = 1/(1+a\gamma^b)$	a	0.172	0.302
	b	1.39	1.57

STRAIN AND TIME DEPENDENCE OF CORRECTION FACTOR

The correction method for the parallel-disk experiments does *not* require separability of time and strain dependence as discussed above. The method can actually be used to check experimentally the separability assumption [Eq. (15)] which is not generally accepted.[22,23] In the following, we discuss what is implied about the correction factor $\chi(t,\gamma_R)$ when one considers the separability assumption and compares the results with experimental findings.

The apparent relaxation modulus defined in Eq. (11) can be rewritten substituting Eq. (8) for the torque and Eq. (15) for $G(t,\gamma)$:

$$G_a(t,\gamma_R) = \mathring{G}(t)\underbrace{\frac{4}{\gamma_R^4}\int_0^{\gamma_R} h(\gamma)\gamma^3\,d\gamma}_{f(\gamma_R)}. \tag{19}$$

It is then factorable into functions of time, $\mathring{G}(t)$, and of strain, $f(\gamma_R)$. Upon differentiation with respect to γ_R,

$$\frac{\partial \ln G_a(t,\gamma_R)}{\partial \ln \gamma_R} = \underbrace{\frac{\partial \ln \mathring{G}(t)}{\partial \ln \gamma_R}}_{0} + \frac{\partial \ln f(\gamma_R)}{\partial \ln \gamma_R}, \tag{20}$$

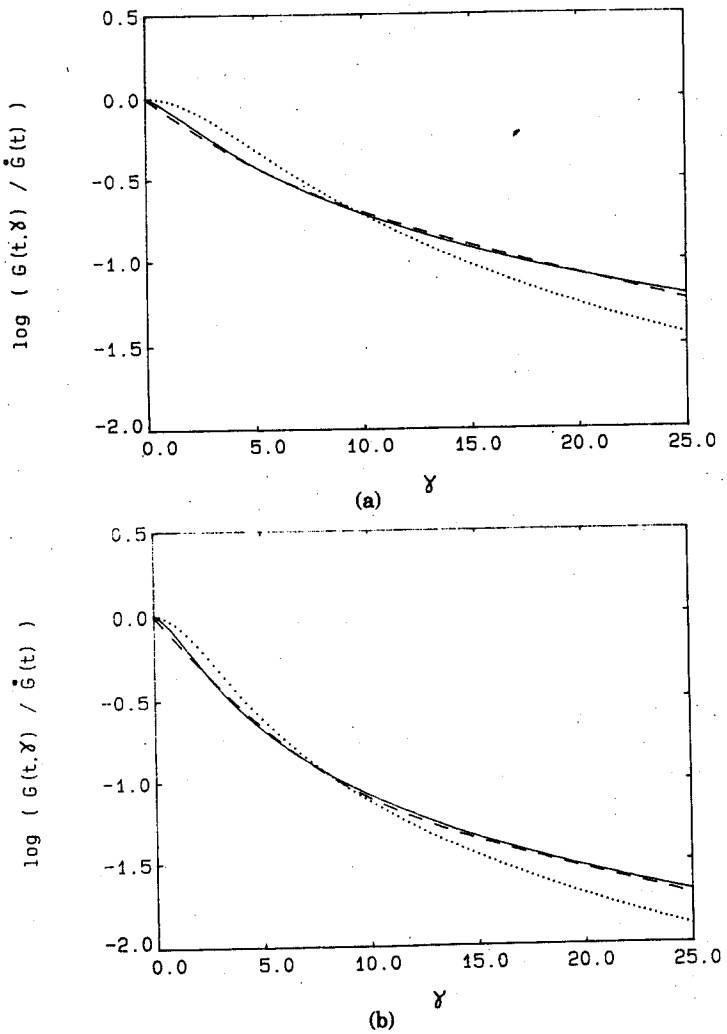

Fig. 10. Predictions of the strain function according to the three approximation functions discussed in the text and the parameters in Table III. (---) from Eq. (16), (···) from Eq. (17) and (—) from Eq. (18). (a) LDPE, T = 150°C, (b) PS, T = 180°C.

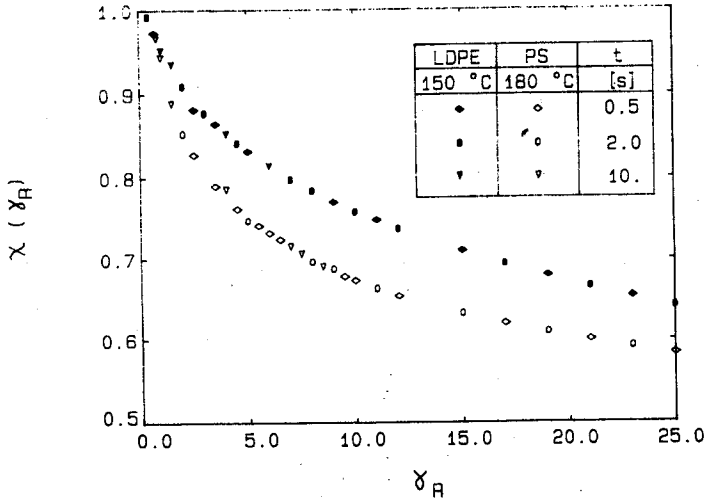

Fig. 11. Correction factor χ as a function of strain for LDPE, T = 150°C (filled symbols) and PS, T = 180°C (open symbols).

we find that the correction factor [Eq. (12)] becomes

$$\chi(\gamma_R) = 1 + \frac{1}{4}\frac{d \ln f(\gamma_R)}{d \ln \gamma_R} = h(\gamma_R)\gamma_R^4 \left(4\int_0^{\gamma_R} h\gamma^3 d\gamma\right)^{-1} \qquad (21)$$

and is *independent of time.*

This independence of time is verified experimentally with the data of Figure 5. The slope of the curves at various times is the same for a particular strain magnitude. The correction factor as a function of strain appears in Figure 11 and is seen to be independent of time from 0.5 to 10 s. Some deviations at times above 10 s were found in the data due to the uncertainty of G_a at long times.

Figure 11 also shows that the correction factor qualitatively gives the same information about the strain dependence of the polymer as the strain function (i.e., the PS has a stronger dependence on large shear strains than the LDPE). The independence of χ on time supports the validity of the separability of the relaxation modulus into time- and strain-dependent functions and also demonstrates that the correction method is applicable to transient experiments of this type.

CONCLUSIONS

Large step shear strain experiments in a parallel-disk rotational rheometer were performed on two polymer melts. A correction method to obtain the shear relaxation modulus at large strains was developed and the data obtained with the parallel-disk geometry agrees with the cone-and-plate data obtained on the same machine. The correction method is straightforward and easy to use.

The correction method for parallel-disk rheometers has the following two applications: First, it allows one to obtain large step strain data from rotational rheometers having a limited angular displacement, and second, the rise times for the step in strain are very short even at large strains due to the smaller angular displacement required. With suitable choices of plate separation H, the rise time can be made the same for all strains (about 50 ms, see Fig. 4).

Information about material behavior was also obtained from the correction factor χ. For both linear (PS) and long chain branched (LDPE) polymers, the correction factor was found to depend on strain only and to be independent of time. This result demonstrates the validity of the correction method for these transient experiments and supports the separability assumption. Also, the correction factor qualitatively gives the same information about the strain dependence of the material as the strain function h.

The strain function $h(\gamma)$ is equally well approximated with a sum of exponential functions and with a sigmoidal function with a strain exponent of about 1.5.

The support through NSF Grant CPE 82-03272 and through Contract N00014-82-K-0083 of the Office of Naval Research is gratefully acknowledged. We also wish to thank E.I. duPont de Nemours & Co. and the Dow Chemical Co. for supplying the polymer samples used in this work.

References

1. L. J. Zapas and J. C. Phillips, *J. Res. Natl. Bur. Stand. USA*, **75A**, 33 (1971).

2. Y. Einaga, K. Osaki, M. Kurata, S. Kimura, N. Yamada, and M. Tamura, *Polym. J.*, **5**, 91 (1973).

3. A. S. Lodge and J. Meissner, *Rheol. Acta,* **11,** 351 (1972).
4. H. M. Laun, *Rheol. Acta,* **17,** 1 (1978).
5. K. Osaki, N. Bessho, T. Kojimoto, and M. Kurata, *J. Rheol.,* **23,** 617 (1979).
6. S. Kimura, K. Osaki, and M. Kurata, *J. Polym. Sci. Polym. Phys. Ed.,* **19,** 151 (1981).
7. K. Osaki, S. Kimura, and M. Kurata, *J. Polym. Sci. Polym. Phys. Ed.,* **19,** 517 (1981).
8. J. D. Ferry, *Viscoelastic Properties of Polymers,* Wiley, New York, 1980.
9. M. Fukuda, K. Osaki, and M. Kurata, *J. Polym. Sci. Polym. Phys. Ed.,* **13,** 1563 (1975).
10. K. Osaki, N. Bessho, T. Kojimoto, and M. Kurata, *J. Rheol.,* **24,** 125 (1980).
11. Y.-H. Lin, *J. Rheol.,* **28,** 1 (1984).
12. K. Osaki, N. Bessho, T. Kojimoto, and M. Kurata, *J. Rheol.,* **23,** 457 (1979).
13. J. Meissner, *J. Appl. Polym. Sci.,* **16,** 2877 (1972).
14. B. Rabinowitsch, *Z. Phys. Chem.,* **A145,** 1 (1929).
15. R. B. Bird, R. C. Armstrong, and O. Hassager, *Dynamics of Polymeric Liquids, Vol. 1,* Wiley, New York, 1977.
16. D. W. Marquardt, *J. SIAM,* **11,** 2 (1963).
17. P. R. Bevington, *Data Reduction and Error Analysis for the Physical Sciences,* McGraw-Hill, New York, 1969, p. 134.
18. M. Doi and S. F. Edwards, *J. Chem. Soc. Faraday Trans. II,* **74,** 1789 (1978); **74,** 1802 (1978); **74,** 1818 (1978); **75,** 38 (1979).
19. M. H. Wagner, *Rheol. Acta,* **15,** 136 (1976).
20. K. Osaki, *Proc. VIIIth Int. Congr. Rheol.,* Gothenburg, 1976, p. 104.
21. A. C. Papanastasiou, L. E. Scriven, and C. W. Macosko, *J. Rheol.,* **27,** 387 (1983).
22. C. M. Vrentas and W. W. Graessley, *J. Rheol.,* **26,** 359 (1982).
23. E. V. Menezes and W. W. Graessley, *J. Polym. Sci. Polym. Phys. Ed.,* **20,** 1817 (1982).

Received October 13, 1983
Accepted as revised January 31, 1984